AMERICAN ACADEMY OF OPHTHALMOLOGY®

Photovoltaic Restoration of Central Vision in Atrophic Age-Related Macular Degeneration

Daniel Palanker, PhD,[1] *Yannick Le Mer, MD,*[2] *Saddek Mohand-Said, MD,*[3,7] *Mahiul Muqit, PhD, FRCOphth,*[4,5] *Jose A. Sahel, MD*[2,3,6]

Purpose: Loss of photoreceptors in atrophic age-related macular degeneration results in severe visual impairment, although some peripheral vision is retained. To restore central vision without compromising the residual peripheral field, we developed a wireless photovoltaic retinal implant (PRIMA; Pixium Vision, Paris, France) in which pixels convert images projected from video glasses using near-infrared light into electric current to stimulate the nearby inner retinal neurons.

Design: We carried out a first-in-human clinical trial to test the safety and efficacy of the prosthesis in patients with geographic atrophy (ClinicalTrials.gov identifier, NCT03333954).

Participants: Five patients with geographic atrophy zone of at least 3 optic disc diameters, no foveal light perception, and best-corrected visual acuity of 20/400 to 20/1000 in the worse-seeing study eye.

Methods: The 2-mm wide, 30-μm thick chip, containing 378 pixels (each 100 μm in diameter), was implanted subretinally in the area of atrophy (absolute scotoma).

Main Outcome Measures: Anatomic outcomes were assessed with fundus photography and OCT for up to 12 months of follow-up. Prosthetic vision was assessed by mapping light perception, bar orientation, letter recognition, and Landolt C acuity.

Results: In all patients, the prosthesis was implanted successfully under the macula, although in 2 patients, it was implanted in unintended locations: within the choroid and off center by 2 mm. All 5 patients could perceive white-yellow prosthetic visual patterns with adjustable brightness in the previous scotomata. The 3 with optimal placement of the implant demonstrated prosthetic acuity of 20/460 to 20/550, and the patient with the off-center implant demonstrated 20/800 acuity. Residual natural acuity did not decrease after implantation in any patient.

Conclusions: Implantation of the PRIMA did not decrease the residual natural acuity, and it restored visual sensitivity in the former scotoma in each of the 5 patients. In 3 patients with the proper placement of the chip, prosthetic visual acuity was only 10% to 30% less than the level expected from the pixel pitch (20/420). Therefore, the use of optical or electronic magnification in the glasses as well as smaller pixels in future implants may improve visual acuity even further. *Ophthalmology 2020;127:1097-1104 © 2020 by the American Academy of Ophthalmology. This is an open access article under the CC BY license (http://creativecommons.org/licenses/by/4.0/).*

Supplemental material available at www.aaojournal.org.

Age-related macular degeneration (AMD) is a leading cause of irreversible vision loss, affecting more than 8.7% of the population worldwide; the number of affected persons is projected to reach 196 million by 2020.[1] Advanced forms of AMD (neovascularization and geographic atrophy) are associated with severe visual impairment, and their prevalence dramatically increases with age: from 1.5% in the United States population older than 40 years to more than 15% in the population older than 80 years.[2]

Geographic atrophy, which occurs at an advanced stage of the disease, results in gradual loss of photoreceptors in the central macula (which is responsible for high-resolution vision) and severely impairs reading and face recognition. Low-resolution peripheral vision is retained in this condition, necessitating the use of eccentric fixation. Therefore, the goal of any treatment strategy should be to provide functional central vision without jeopardizing the surrounding retina.

Although photoreceptors in retinal degeneration are lost, the inner retinal neurons survive to a large extent.[3–5] Electronic retinal prostheses are designed to reintroduce visual information into the degenerate retina by electrical stimulation of the remaining neurons. Current strategies involve placing electrode arrays either subretinally, to stimulate the first layer of neurons above the photoreceptor cells (mainly bipolar cells in the inner nuclear layer[6–8]), or epiretinally, to target the retinal ganglion cells.[9,10] The epiretinal implant (ARGUS II; Second Sight Inc, Sylmar, CA) currently approved for patients blinded by inherited retinal degeneration (retinitis pigmentosa [RP]) has 60 electrodes (200 μm in diameter, 575 μm pitch)[11] that are relatively distant (on average, approximately 180 μm)

https://doi.org/10.1016/j.ophtha.2020.02.024
ISSN 0161-6420/20

from the target retinal ganglion cells.[12] Patients using this system have been reported to have low visual acuity, of 20/1260 or worse.[13] In addition to activation of proximal neurons, this implant stimulates the axons of remote retinal ganglion cells passing underneath the electrodes, causing distorted visual percepts.[14]

Preclinical studies in rodents demonstrated that stimulation of bipolar cells via subretinal implants results in a network-mediated retinal response that preserves many features of normal vision: flicker fusion at high frequencies (>20 Hz)[15,16] and adaptation to static images,[17] "on" and "off" responses to increments and decrements in light with antagonistic center-surround organization,[18] and nonlinear summation of the inputs from bipolar cells into ganglion cells' receptive fields (so-called subunits),[16] essential for high spatial resolution.

A subretinal implant, the Alpha IMS/AMS (Retina Implant AG, Reutlingen, Germany), having up to 1600 pixels, each of 70 μm in width, was tested in patients blinded by RP. Of 44 trial participants, visual acuity using Landolt C was measurable in 6 patients, ranging from 20/2000 to 20/546 (2 patients).[19,20] None of the trials' participants achieved an acuity approaching the theoretical limit of resolution of the pixel array, approximately 20/280. This could be because of the monopolar design of this implant, in which active electrodes share a common remote return electrode, an arrangement that may result in strong so-called cross-talk between neighboring electrodes, and thus may limit spatial contrast.[21] It is also possible that the highly remodeled retinal neural network in advanced stages of RP[22] degrades the attainable prosthetic acuity in such patients.

Both of these implants are powered via a transscleral cable inserted in complex surgical procedures that is associated with postoperative complications[13,19] that may affect residual peripheral vision, an especially important concern for patients with AMD.

We developed a wireless prosthesis in which photovoltaic pixels directly convert projected light patterns into local electric current.[8,16] It is 2 mm in width (corresponding to approximately 7° of the visual angle in a human eye), 30 μm in thickness, with 378 pixels, each of which is 100 μm in diameter (PRIMA [Pixium Vision, Paris, France]; Fig 1). Images captured by the camera are processed and projected onto the retina from video glasses using near-infrared (880 nm) light to avoid photophobic and phototoxic effects of bright illumination.[23] Current flowing through the retina between the local active and return electrodes stimulates the nearby inner retinal neurons,[8] which then pass the responses to ganglion cells, thereby harnessing some of the residual retinal signal processing.[16,18,24] To avoid irreversible electrochemical reactions at the electrode−electrolyte interface, stimulation is charge balanced, and hence it is pulsed with alternating polarity.[25] For continuous perception under pulsed illumination, we apply sufficiently high frequencies to enable flicker fusion. Preclinical studies in rodents demonstrated retinal adaptation to frequencies exceeding 20 Hz under network-mediated stimulation.[16,26] Localization of the electric field is achieved by providing active and return electrodes in each pixel.[16] In preclinical testing in rodents, such photovoltaic arrays with pixels of 75 μm and 55 μm in width provided grating visual acuity (alternating light and dark stripes) matching the pixel density.[16,26] Preclinical testing of the PRIMA implants having 100-μm pixels in nonhuman primates demonstrated similar stimulation thresholds to those observed in rodents and perceptual responses (saccadic movement) down to a single pixel activation.[27]

Methods

Patients

The aim of this first-in-human feasibility study of the PRIMA implant (ClinicalTrials.gov identifier, NCT03333954) was to test safety and functionality of this device in 5 patients with AMD. The study adhered to the tenets of the Declaration of Helsinki and received ethics committee approval from the Comité de Protection des Personnes Ile de France II and the Agence Nationale de Sécurité du Médicament et des Produits de Santé. Study participants were older than 60 years and had advanced dry AMD with an atrophic zone of at least 3 optic disc diameters and best-corrected visual acuity of 20/400 or worse in the worse-seeing study eye; no foveal light perception (absolute scotoma), but visual perception in the periphery, with preferred retinal locus determined by microperimetry; absence of photoreceptors and presence of the inner retina in the atrophic area as confirmed by OCT; and absence of choroidal neovascularization verified by retinal angiography. All other ocular and general pathologic features that could contribute to the low visual acuity were excluded. Patients provided written informed consent to participate in the study.

Surgery

Surgical procedures were performed in the Fondation Ophtalmologique A. de Rothschild (Paris, France) under local or general anesthesia. The study eye was prepared for surgery with antiseptic solution. Complete 23-gauge vitrectomy and removal of the posterior hyaloid was performed. The macula was detached with a subretinal injection of balanced salt solution via a 42-gauge needle inserted at a position away from the preferred retinal locus to avoid damage to the residual useful vision. A retinotomy (of approximately 2.5 mm) was performed at the margin of the atrophic area with vertical scissors, and if not totally detached by the balanced salt solution injection, the neural retina was dissected from the underlying atrophic pigment epithelium with a subretinal pick or spatula. A 2.4-mm sclerotomy then was created for intraocular implant delivery. The implant was inserted under the neural retina using silicone-coated forceps and placed near the target location under the retina. The implant then was guided to the desired central location by application of soft touch over the retina. Perfluorocarbon liquid was injected over the posterior pole to stabilize the implant and then removed via fluid-to-air exchange. Intraoperative OCT was used to verify retinal flattening, and the air was exchanged with a tamponade agent, either silicone oil or gas. In patients 1, 2, and 3, the air was exchanged with silicone oil (which was removed under local anesthesia 1 month later), and in patients 4 and 5, the air was exchanged with gas (hexafluoroethane and sulfur hexafluoride, respectively), and the 2.4-mm sclerotomy was closed.

After surgery, the patients were prescribed the usual postoperative topical treatment with a combination of dexamethasone and tobramycin eye drops 3 times daily for 4 weeks. Patients 4 and 5, who received an air−gas exchange, received 250 mg of acetazolamide 1 and 6 hours after surgery and assumed a prone position for 12 hours after surgery.

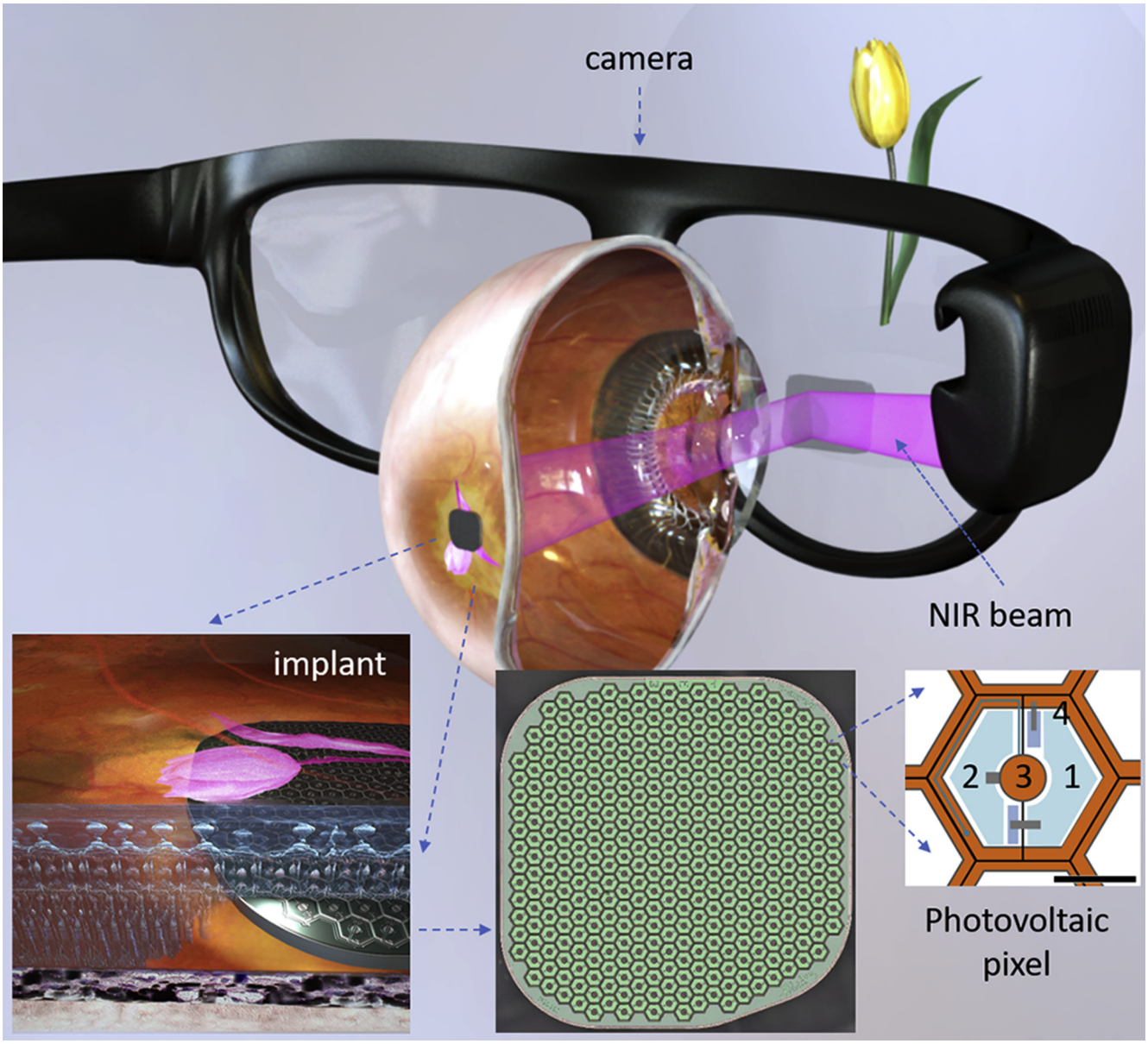

Figure 1. System diagram showing the photovoltaic retinal prosthesis, including the camera integrated into augmented reality–like video glasses, with the processed image projected onto the retina using pulsed near-infrared (NIR) light. Subretinal wireless photovoltaic array converts pulsed light into pulsed electric current in each pixel to stimulate the adjacent inner retinal neurons. Each pixel includes 2 diodes (1 and 2), connected in series between the active (3) and return (4) electrodes. Scale bar = 50 μm.

Assessment of Prosthetic Vision

The patients' rehabilitation and visual function assessment were carried out at the Clinical Investigation Center of Quinze-Vingts National Eye Hospital (Paris, France). To assess prosthetic vision independently of remaining natural vision, we made use of opaque video glasses with a Digital Mirror Display in front of the operated eye (Fig 2) . The projected images cover a field of 5.1 mm (17°) on the retina, with resolution of 10.5 μm. Maximum peak retinal irradiance was 3 mW/mm^2, well within the thermal safety limits for chronic use of near-infrared light.[28] Brightness of the percept was controlled by pulse duration of between 0.7 and 9.8 ms, in 0.7-ms steps. The glasses also included a miniature video camera, allowing patients to see a video stream of the visual scene captured by the camera (Fig 2). Alternatively, the system can project computer-generated images into the eye. The camera captured a visual field of 50° × 40°, but only the central one third of the image was projected onto the retina to match the 17° field of view of the display. Thus, the angular magnification of the system was 1:1, that is, no optical or electronic zoom was used for acuity measurements or letter recognition.

Visual acuity was assessed using a computer-generated Landolt C chart in 4 different orientations (gap at the top, bottom, right, or left), so that a random response corresponds to 25% accuracy. The minimum optotype size was defined as the proper symbol recognition with at least 62.5% accuracy. To minimize the number of presentations, the study was conducted similarly to the Freiburg vision test.[29]

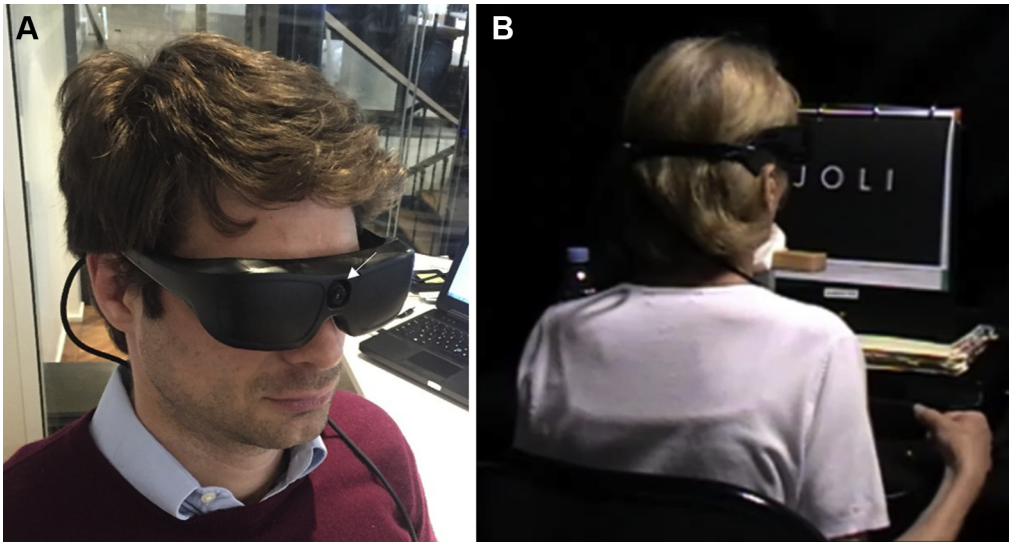

Figure 2. **A**, Photograph showing the opaque video glasses with an integrated camera (white arrow) used in the feasibility study. **B**, Photograph showing letter recognition and reading tests with one of the patients, using the camera mode.

For the letter recognition test, the alphabet was split into 3 groups of increasing difficulty, as applied previously in assessment of prosthetic vision:[30] set A comprised L, T, E, F, J, H, I, and U; set B comprised A, Z, Q, V, N, W, O, C, D, and M; and set C comprised K, R, G, X, B, Y, S, and P. The overall methodology of the test (forced-choice, closed-set, with 4 repetitions of each letter) also matched the previous study,[30] except that we used smaller letters of 2.8 cm at a distance of 30 cm.

Results

Following screening of the patient database at the Rothchild Foundation and Quinze-Vingts National Eye Hospital, those who met the inclusion criteria were invited to participate. The first patient was enrolled on November 13, 2017, and the last patient was enrolled on May 25, 2018. The 12-month examinations were completed on June 14, 2019.

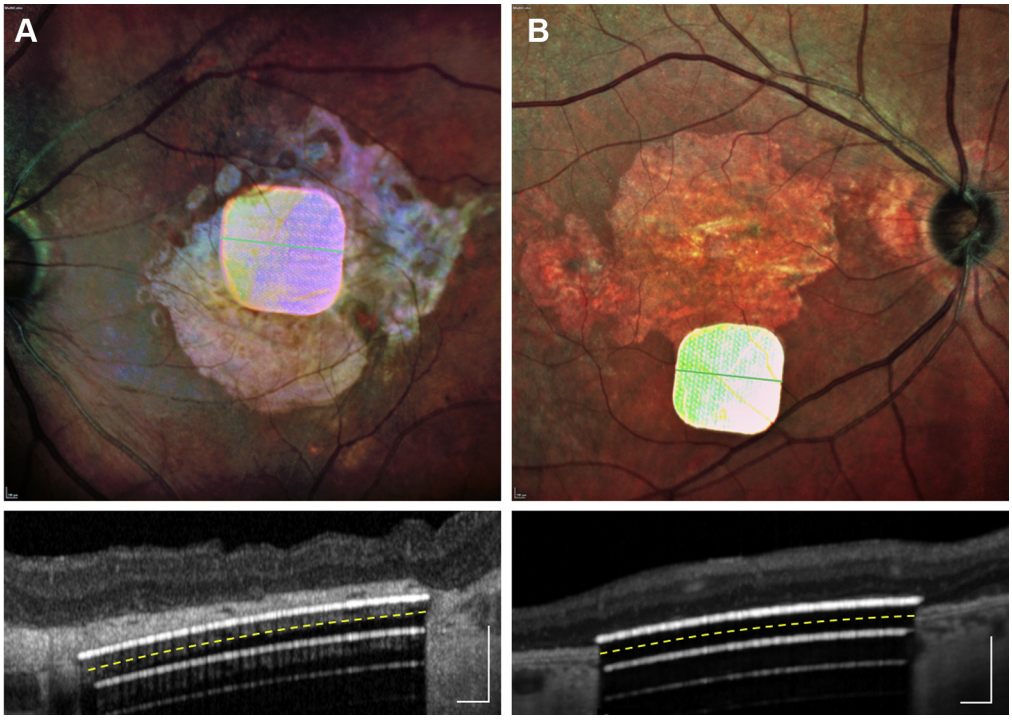

Figure 3. Fundus photographs and OCT images obtained along the green line, with 2 implants in unintended locations: (**A**) in the choroid in patient 1 and (**B**) in the periphery of the macula in patient 4. Yellow dashed line indicates the back side of the implant. White lines underneath the implant are the OCT reflections. Images were obtained during the 6-week to 6-month postoperative visits. Scale bars = 200 μm.

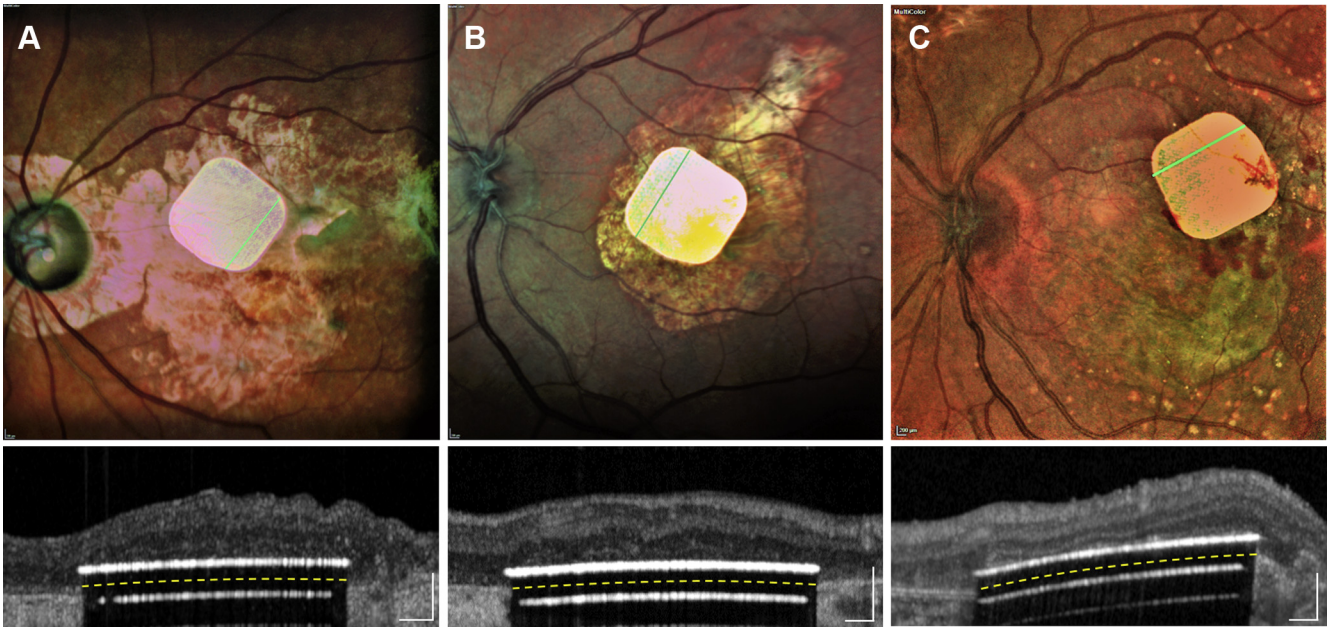

Figure 4. Fundus photographs and OCT images with 3 implants in intended locations: (**A**) patient 2, (**B**) patient 3, and (**C**) patient 5. Images were obtained during the 6-week to 6-month postoperative visits.

Surgical Placement of Implant

Patient 1, who underwent surgery under local anesthesia, moved when the implant was held by forceps under the retina, provoking inadvertent insertion of the chip into the choroid, accompanied by bleeding from the choroid that was evacuated partially during surgery. The blood resolved within 6 months, but an OCT image obtained at 6 months (Fig 3A) demonstrated that the chip was separated from the inner nuclear layer by a hyperreflective layer of approximately 70 μm in thickness. This layer could be a choroid, scar tissue that formed above the chip in response to choroidal injury, or both. For all other patients (patients 2–5), surgery was performed under general anesthesia.

In 2 other patients, focal subretinal bleeding occurred from the retinal vessels at the retinotomy site, remaining at a distance from the implant and resolving within a few weeks. One patient with a gas exchange (patient 4) moved his head from the prone position immediately after surgery, before the retina had fully re-adhered. As a result, the chip shifted by approximately 2 mm from its initial location in the center of the geographic atrophy area, although it remained in the scotoma (Fig 3B). The same patient did not take the prescribed medication (250 mg acetazolamide) after surgery, resulting in acute increase of intraocular pressure. This was treated successfully with intravenous acetazolamide, followed by β-blocker eyedrops for 1 week. In patients 2, 3, and 5, the implant remained stable, in a central location, and in close proximity to the inner retina (Fig 4). The mean surgical time for all 5 implantations was 2 hours and 4 minutes, ranging from 1 hour and 57 minutes to 2 hours and 10 minutes.

Over the 12 months after surgery, the implants remained in the same location under the retina. To assess the effect of separation between electrodes and neurons on visual acuity and stimulation threshold, we measured the average distance between the chip and the bottom of the inner nuclear layer in each patient at 3, 6, and 12 months after surgery (Table 1). In patients with subretinal placement of the implant (patients 2–5), the average distance between the inner nuclear layer and implant was 35 to 39 μm at 12 months.

Natural Vision

Residual natural visual acuity in the treated eye did not decrease in any patient during the follow-up period (Table 1). In fact, it improved slightly in patients 1, 3, 4, and 5. This could be either the result of neurotrophic benefit of the subretinal surgery or of the electrical stimulation,[31] or a result of the vision rehabilitation training, which has the potential to improve preferred eccentric fixation.

Prosthetic Vision

In each patient, we first determined the perceptual threshold in terms of pulse duration using a 16-pixels-wide circular spot at a 10-Hz repetition rate, presented for up to 20 seconds at 3 mW/mm^2 irradiance (Table 1). Thresholds were determined with adaptive Best PEST (Parameter Estimation by Sequential Testing) procedure[32] of 15 to 20 repetitions. A strength-duration curve also was measured in each patient, from which the chronaxie and rheobase were computed. All patients described the percepts as bright white-yellow phosphenes inside the scotoma. At maximum pulse duration (9.8 ms), each patient described the percept as being as bright as a desk reading lamp. When we increased pulse frequency from 3 to 10 Hz, all patients reported that percepts were more persistent. Flickering decreased further when the frequency was increased to 30 Hz and disappeared completely at 60 Hz. When tested in the dark, the patients sometimes could see the 880-nm radiation as a faint red light in the periphery. Therefore, during vision tests, all patients were asked about the color of percepts to ensure that only the white-yellow percepts were considered. Stimulation thresholds and perceptual brightness remained stable during the follow-up of the study.

In the visual field test (Octopus 900; Haag-Streit, Koniz, Switzerland) at 6 and 12 months, all 5 patients reported light perception in the atrophic zone, elicited by the implant when the system was turned on, and no perception when the system was turned off. At the 12-month test, patient 5 reported also sometimes

Table 1. Residual Natural Vision, Anatomic, and Functional Outcomes with the Implant

Test	Patient No. 1	2	3	4	5
Residual peripheral vision					
Preoperative eccentric natural acuity in the study eye	20/400 (1.3 logMAR)	20/800 (1.6 logMAR)	20/1000 (1.7 logMAR)	20/500 (1.4 logMAR)	20/500 (1.4 logMAR)
Postoperative eccentric natural acuity in the study eye (12 mos)	20/320 (1.2 logMAR)	20/800 (1.6 logMAR)	20/800 (1.6 logMAR)	20/400 (1.3 logMAR)	20/400 (1.3 logMAR)
Implant location					
Implant location in the macula	Intrachoroidal	Central subretinal	Central subretinal	Off-center subretinal	Central subretinal
Average distance from implant to bottom of INL (μm)					
3 mos	127	34	43	37	51
6 mos	103	28	35	38	39
12 mos	138	39	39	35	37
Perceptual stimulation thresholds					
Chronaxie (ms)	NA	2.5	2.3	2.2	2.1
Rheobase (mW/mm^2)	NA	1.0	0.4	1.4	0.5
Threshold pulse duration (ms) for 3 mW/mm^2	2.1	0.8	0.7	1.0	0.8
Central vision					
Natural central visual perception	None	None	None	None	None
Prosthetic bar orientation, % correct (95% CI)	28 (20–40)	96 (93–98)	96 (93–98)	94 (86–98)	88 (75–95)
Prosthetic minimum bar width on retina, pixels (% correct), (95% CI)	2 (90), (55–100)	1 (100), (69–100)	1 (70), (35–93)	1 (50), (19–82)	1 (80), (44–97)
Prosthetic central acuity	Light perception	20/550 (1.44 logMAR)	20/500 (1.4 logMAR)	20/800 (1.6 logMAR)	20/460 (1.37 logMAR)
Minimum Landolt C gap (pixels)		1.3	1.2	1.9	1.1

CI = confidence interval; INL = inner nuclear layer; logMAR = logarithm of the minimum angle of resolution.

experiencing a phantom visual perception not elicited by visual or electrical stimulation[33] when the device was turned off.

Tests with the computer-generated images defined the minimum width of a visible bar to be 1 pixel for patients 2 through 5, with the population average of identification of 75±20% ($P = 0.002$; 95% confidence interval, 59%–87%), and 2 pixels for patient 1, with 90% identification ($P = 0.021$; 95% confidence interval, 55%–100%). In the forced-choice bar orientation test (vertical, horizontal, and 2 diagonals in opposing directions), patients 2, 3, 4, and 5 achieved 93.5±3.8% accuracy. Patient 1, in whom the implant was placed in the choroid, identified the correct orientation with 28% accuracy, consistent with no improvement when using prosthetic vision (Table 1). Patients described the bars presented in various orientations as straight lines or elongated objects, demonstrating correct retinotopy of perception.

The 3 patients with optimal placement of the implant (patients 2, 3, and 5) demonstrated visual acuity with the Landolt C chart in the range of 20/460 to 20/550 (1.37–1.44 logarithm of the minimum angle of resolution) within 12 months, which is 10% to 30% less than the theoretical resolution limit (Nyquist sampling limit) for this pixel size (20/420, assuming 10° of the visual angle corresponds to 288 μm on the retina[34]). Patient 4 demonstrated prosthetic acuity of 20/800 (1.6 logarithm of the minimum angle of resolution), whereas patient 1 could not resolve letters or optotypes of any size (Table 1). The population average prosthetic logarithm of the minimum angle of resolution acuity was 1.45±0.10, with the 95% confidence interval of 1.29 to 1.62, calculated based on t distribution.

We asked patient 2 to recognize letters of 2.8 cm in height positioned 30 cm away from the face. This patient identified group A letters with 88% accuracy and 8-second median response time, group B letters with 80% accuracy and 7-second median response time, and group C letters with 75% accuracy and 11-second median response time. Letter recognition did not involve the head scanning, but rather, just the eye scanning of the image (Video 1, available at www.aaojournal.org). This patient was able to read words, as illustrated in the same video. As a control, when the system was turned off, the patient had no visual perception because the opaque glasses used in these tests blocked the residual natural vision (Video 2, available at www.aaojournal.org).

Discussion

The wireless nature of the PRIMA implant greatly simplifies the surgical procedures compared with the wired retinal prostheses. All the procedures in PRIMA surgery can be performed within 2 hours, as opposed to approximately 4 hours with the Argus II[13] and 6 to 8 hours with the Alpha IMS.[19] The most challenging part of the surgery is to separate the retina from retinal pigment epithelium–choroid in atrophic macula, which often requires not only subretinal injection of fluid, but also careful delamination with a spatula. Implant release from the forceps in the intended location under the retina also is not trivial. To simplify this step in the procedure, we developed an injector of the implant, which will be used in future trials. To avoid potential movement of patients in a wrong moment, as occurred with patient 1, we

recommend performing the surgery under general anesthesia, if possible, or to ask patients to keep steady at critical moments. Patient compliance regarding the prone head position after the gas exchange procedure is essential, because otherwise the implant can shift from the original location before complete retinal reattachment, as was seen with patient 4.

Spatial resolution in patterned retinal stimulation depends not only on the pixel size, but also on the distance between electrodes and target neurons.[35] Ideally, for localized and efficient stimulation, it should not exceed the pixel radius. In patients 2 through 5, the distance between the inner nuclear layer and the implant was approximately 35 to 39 μm, smaller than the 50-μm radius of the current pixels (Table 1). However, in patient 1, it exceeded 100 μm, which may explain the suboptimal performance of this patient.

From preclinical studies in rodents, we knew that many features of the retinal signal processing are preserved with subretinal prosthetics, such as flicker fusion at high frequencies,[15,16] on and off responses with antagonistic center surround,[18] and nonlinear summation of the inputs from bipolar cells into ganglion cells' receptive fields.[16] However, we did not know what the actual human perception with such prosthesis would be. One of the most striking aspects of these clinical observations is that perception of prosthetic vision was remarkably natural, that is, as soon as patients learned how to use the video glasses, the prosthetic line patterns appeared in a correct shape right away, without scanning. Despite the likely indiscriminate electrical activation of multiple cell types in the inner retina (on and off, for example), our patients reported correct form perception of bright patterns (lines, letters, etc.) on a dark background. This may indicate that either the excitatory pathways dominate the perception, or that the brain filters out conflicting inputs and correctly interprets the images even when the signal encoding deviates from natural.

One reason for better and more consistent performance of the patients in the current trial compared with previous trials with a subretinal implant may be patient selection: AMD patients may have much better-preserved inner retina in the relatively small central scotoma than at the end stage of RP, associated with a long-lasting and nearly complete loss of photoreceptors in the entire retina. Animal studies of the retinal remodeling in inherited retinal degeneration indicate that massive retinal reorganization occurs only when nearly all the photoreceptors are gone,[22,36] a situation that does not occur in AMD patients.

In summary, within the limits of a small study, we demonstrated that submacular implantation of a wireless photovoltaic array in patients with geographic atrophy is feasible, that the implant is stable over time, and that it did not decrease the eccentric natural acuity. All 4 patients with subretinal placement of the chip achieved letter acuity. In 3 patients with central chip placement, prosthetic acuity was only 10% to 30% less than the sampling limit for the current pixel size. The use of optical or electronic magnification in future glasses or implants with smaller pixels may improve the prosthetic visual acuity further. As the next step, we will test the transparent (augmented reality) glasses to allow simultaneous use of the prosthetic central and natural peripheral vision, which should improve the benefit of the PRIMA system in daily living.

Acknowledgments

The authors thank the patients who participated in the study; the Pixium Vision team who designed, fabricated, and tested the PRIMA system; the Scientific and Medical Advisory Board of Pixium Vision for its guidance on the clinical trial design; and all the scientific, research and development, medical, and clinical research staff who continue the patient care, rehabilitation, and evaluation.

References

1. Wong WL, Su X, Li X, et al. Global prevalence of age-related macular degeneration and disease burden projection for 2020 and 2040: a systematic review and meta-analysis. *Lancet Glob Health*. 2014;2:e106–e116.
2. Friedman DS, Tomany SC, McCarty C, De Jong P. Prevalence of age-related macular degeneration in the United States. *Arch Ophthalmol*. 2004;122:564–572.
3. Mazzoni F, Novelli E, Strettoi E. Retinal ganglion cells survive and maintain normal dendritic morphology in a mouse model of inherited photoreceptor degeneration. *J Neurosci*. 2008;28:14282–14292.
4. Humayun MS, Prince M, de Juan E, et al. Morphometric analysis of the extramacular retina from postmortem eyes with retinitis pigmentosa. *Invest Ophthalmol Vis Sci*. 1999;40:143–148.
5. Kim SY, Sadda S, Pearlman J, et al. Morphometric analysis of the macula in eyes with disciform age-related macular degeneration. *Retina*. 2002;22:471–477.
6. Zrenner E. Fighting blindness with microelectronics. *Sci Transl Med*. 2013;5:210ps16. https://doi.org/10.1126/scitranslmed.3007399.
7. Zrenner E, Bartz-Schmidt KU, Benav H, et al. Subretinal electronic chips allow blind patients to read letters and combine them to words. *Proc Biol Sci*. 2011;278:1489–1497.
8. Mathieson K, Loudin J, Goetz G, et al. Photovoltaic retinal prosthesis with high pixel density. *Nat Photonics*. 2012;6:391–397.
9. Behrend MR, Ahuja AK, Humayun MS, et al. Resolution of the epiretinal prosthesis is not limited by electrode size. *IEEE Trans Neural Syst Rehabil Eng*. 2011;19:436–442.
10. Jensen RJ, Rizzo 3rd JF. Thresholds for activation of rabbit retinal ganglion cells with a subretinal electrode. *Exp Eye Res*. 2006;83:367–373.
11. Luo YH-L, da Cruz L. The Argus® II retinal prosthesis system. *Prog Retin Eye Res*. 2016;50:89–107.
12. Ahuja AK, Yeoh J, Dorn JD, et al. Factors affecting perceptual threshold in Argus II retinal prosthesis subjects. *Transl Vis Sci Technol*. 2013;2:1.
13. Humayun MS, Dorn JD, da Cruz L, et al. Interim results from the international trial of Second Sight's visual prosthesis. *Ophthalmology*. 2012;119:779–788.
14. Nanduri D, Fine I, Horsager A, et al. Frequency and amplitude modulation have different effects on the percepts elicited by retinal stimulation. *Invest Ophthalmol Vis Sci*. 2012;53:205–214.
15. Lorach H, Goetz G, Mandel Y, et al. Performance of photovoltaic arrays in-vivo and characteristics of prosthetic vision in animals with retinal degeneration. *Vision Res*. 2015;111:142–148.
16. Lorach H, Goetz G, Smith R, et al. Photovoltaic restoration of sight with high visual acuity. *Nat Med*. 2015;21:476–482.

17. Stingl K, Bartz-Schmidt KU, Gekeler F, et al. Functional outcome in subretinal electronic implants depends on foveal eccentricity. *Invest Ophthalmol Vis Sci*. 2013;54:7658–7665.
18. Ho E, Smith R, Goetz G, et al. Spatiotemporal characteristics of retinal response to network-mediated photovoltaic stimulation. *J Neurophysiol*. 2017;119:389–400.
19. Stingl K, Bartz-Schmidt KU, Besch D, et al. Subretinal visual implant Alpha IMS—clinical trial interim report. *Vision Res*. 2015;111:149–160.
20. Stingl K, Schippert R, Bartz-Schmidt KU, et al. Interim results of a multicenter trial with the new electronic subretinal implant Alpha AMS in 15 patients blind from inherited retinal degenerations. *Front Neurosci*. 2017;11:445.
21. Loudin JD, Simanovskii DM, Vijayraghavan K, et al. Optoelectronic retinal prosthesis: system design and performance. *J Neural Eng*. 2007;4:S72–S84.
22. Marc RE, Jones BW. Retinal remodeling in inherited photoreceptor degenerations. *Mol Neurobiol*. 2003;28:139–147.
23. Goetz GA, Mandel Y, Manivanh R, et al. Holographic display system for restoration of sight to the blind. *J Neural Eng*. 2013;10(5):056021. https://doi.org/10.1088/1741-2560/10/5/056021.
24. Ho E, Lorach H, Goetz G, et al. Temporal structure in spiking patterns of ganglion cells defines perceptual thresholds in rodents with subretinal prosthesis. *Sci Rep UK*. 2018;8:3145.
25. Boinagrov D, Lei X, Goetz G, et al. Photovoltaic pixels for neural stimulation: circuit models and performance. *IEEE Trans Biomed Circuits Syst*. 2016;10:85–97.
26. Ho E, Lei X, Flores T, et al. Characteristics of prosthetic vision in rats with subretinal flat and pillar electrode arrays. *J Neural Eng*. 2019;16:066027.
27. Prévot P-H, Gehere K, Arcizet F, et al. Behavioural responses to a photovoltaic subretinal prosthesis implanted in non-human primates. *Nat Biomed Eng*. 2020;4:172–180.
28. Lorach H, Wang J, Lee DY, et al. Retinal safety of near infrared radiation in photovoltaic restoration of sight. *Biomed Opt Express*. 2016;7:13–21.
29. Bach M. The Freiburg visual acuity test—automatic measurement of visual acuity. *Optom Vision Sci*. 1996;73:49–53.
30. da Cruz L, Coley BF, Dorn J, et al. The Argus II epiretinal prosthesis system allows letter and word reading and long-term function in patients with profound vision loss. *Br J Ophthalmol*. 2013;97:632–636.
31. Castaldi E, Cicchini GM, Cinelli L, et al. Visual BOLD response in late blind subjects with Argus II retinal prosthesis. *PLoS Biol*. 2016;14:e1002569.
32. Lieberman HR, Pentland AP. Microcomputer-based estimation of psychophysical thresholds—the Best Pest. *Behav Res Meth Instr*. 1982;14:21–25.
33. Pearson J, Westbrook F. Phantom perception: voluntary and involuntary nonretinal vision. *Trends Cogn Sci*. 2015;19:278–284.
34. Drasdo N, Fowler CW. Non-linear projection of the retinal image in a wide-angle schematic eye. *Br J Ophthalmol*. 1974;58:709–714.
35. Palanker D, Vankov A, Huie P, Baccus S. Design of a high resolution optoelectronic retinal prosthesis. *J Neural Eng*. 2005;2:S105–S120.
36. Marc R, Jones B, Anderson J, et al. Neural reprogramming in retinal degeneration. *Invest Ophthalmol Vis Sci*. 2007;48:3364–3371.

Footnotes and Financial Disclosures

Originally received: November 20, 2019.
Final revision: February 14, 2020.
Accepted: February 18, 2020.
Available online: February 25, 2020. Manuscript no. D-19-00763.

[1] Department of Ophthalmology and Hansen Experimental Physics Laboratory, Stanford University, Stanford, California.
[2] Department of Ophthalmology, Fondation Ophtalmologique A. de Rothschild, Paris, France.
[3] Clinical Investigation Center, Quinze-Vingts National Eye Hospital, Paris, France.
[4] Vitreoretinal Service, Moorfields Eye Hospital, London, United Kingdom.
[5] Institute of Ophthalmology, University College London, London, United Kingdom.
[6] Department of Ophthalmology, University of Pittsburgh School of Medicine, Pittsburgh, Pennsylvania.
[7] Sorbonne Université, INSERM, CNRS, Institut de la Vision, Paris, France.

Presented in part at: American Academy of Ophthalmology Annual Meeting, Chicago, Illinois, October 2018; Association for Research in Vision and Ophthalmology Annual Meeting, Vancouver, Canada, May 2019; and EURETINA Annual Meeting, Paris, France, September 2019.

Financial Disclosure(s):

The author(s) have made the following disclosure(s): D.P.: Consultant – Pixium Vision, Topcon Medical Laser Systems, Kedalion Therapeutics; Patents and Royalties – Pixium Vision

Y.L.: Consultant – Pixium Vision, Bausch & Lomb; Lecturer – Allergan. S.M-S.: French state fund LABEX LIFESENSES [ANR-10-LABX-65]; French state fund IHU FOReSIGHT [ANR-18-IAHU-0001].

J.A.S.: Equity owner – Pixium Vision, Gensight Biologics, Sparing Vision, Prophesee, Chronolife, Tilak

Supported by Pixium Vision, Paris, France; the Sight Again Project (via Structural R&D Projects for Competitiveness and Investment for the Future funding managed by Bpifrance); the National Institutes of Health, Bethesda, Maryland (grant no.: R01-EY027786 [D.P.]); the Biomedical Research Centre at Moorfields Eye Hospital, which is supported in part by the National Institute for Health Research, United Kingdom; and the Clinical Investigation Center at the Quinze-Vingts National Hospital, which is supported in part by the Inserm-DHOS, France.

HUMAN SUBJECTS: Human subjects were included in this study. The human ethics committees at the Comité de Protection des Personnes Ile de France II and the Agence Nationale de Sécurité du Médicament et des Produits de Santé approved the study. All research adhered to the tenets of the Declaration of Helsinki. All participants provided informed consent.

No animal subjects were included in this study.

Author Contributions:

Conception and design: Palanker, Le Mer, Mohand-Said, Muqit, Sahel

Analysis and interpretation: Palanker, Le Mer, Mohand-Said, Muqit, Sahel

Data collection: Le Mer, Mohand-Said

Obtained funding: Sahel, Mohand-Said

Overall responsibility: Palanker, Le Mer, Mohand-Said, Sahel

Abbreviations and Acronyms:
AMD = age-related macular degeneration; **RP** = retinitis pigmentosa.

Correspondence:
Daniel Palanker, PhD, Department of Ophthalmology and Hansen Experimental Physics Laboratory, Stanford University, 452 Lomita Mall, Stanford, CA 94305. E-mail: palanker@stanford.edu.